Ionics (2015) 21:125–132
DOI 10.1007/s11581-014-1174-4

ORIGINAL PAPER

Magnesium ion conducting solid polymer blend electrolyte based on biodegradable polymers and application in solid-state batteries

Anji Reddy Polu · Ranveer Kumar · Hee-Woo Rhee

Received: 4 March 2014 / Revised: 26 May 2014 / Accepted: 28 May 2014 / Published online: 8 June 2014

Abstract Magnesium ion conducting solid polymer blend electrolyte based on biodegradable polymers polyvinyl alcohol (PVA) and polyvinyl pyrrolidone (PVP) mixed with different molecular weight percentages (wt.%) of magnesium nitrate ($Mg(NO_3)_2$) was prepared by using solution casting technique. X-ray diffraction studies lead the reduction of crystalline nature by the addition of magnesium nitrate to the polymeric matrix. The complex formation between polymer and salt confirmed by Fourier transform infrared spectroscopy studies. Differential scanning calorimetry shows that the glass transition temperature decreases with increase in magnesium salt concentration and the thermal stability of PVA–PVP–$Mg(NO_3)_2$ complexes. The maximum ionic conductivity $\sigma \sim 3.78 \times 10^{-5}$ S cm^{-1} was obtained for 50PVA–50PVP–30 wt.% of $Mg(NO_3)_2$ polymer blend electrolyte at room temperature (303 K). The conductivity–temperature plot is found to follow the Arrhenius behavior, which showed the decrease in activation energy with the increasing salt concentration. The transference number data indicated the dominance of ion-type charge transport in these polymer blend electrolytes. The solid-state electrochemical cells were fabricated, and their discharge profiles were studied for this polymer blend electrolyte system under a constant load of 100 kΩ.

A. R. Polu (✉) · R. Kumar
Department of Physics, Dr. H S Gour Central University, Sagar, M.P., India 470003
e-mail: reddyphysics06@gmail.com

A. R. Polu · H.-W. Rhee
Department of Chemical and Biomolecular Engineering, Sogang University, Seoul 121-742, South Korea

Keywords Polymer blend · $Mg(NO_3)_2$ · XRD · Ionic conductivity · Electrochemical cell

Introduction

Ionic polymer complexes are scientifically interesting owing to their possible wide range of applications in solid-state electrochemical devices such as energy conversion units (batteries per fuel cells), electrochemical display devices/smart windows, photoelectrochemical cells, etc. [1–4]. The polymer battery has the advantage of having high-energy density, a solvent-free condition,easy processability, and being leak-proof and light weight. The investigations of solid polymer electrolytes have focused on the enhancement of electrical and mechanical properties for their commercial applications in the field of solid-state electrochemical devices. Various methods have been adopted to reduce crystallinity of polymer electrolytes and to increase segmental mobility of host polymer such as blending, copolymerization, cross-linking, and plasticization of matrix polymer [5]. Among the above, blending of polymers is a useful tool to develop new polymeric materials with improved mechanical stability and electrical conductivity. The most common interactions present in blends are hydrogen bonding and ionic and dipole interactions. Main advantages of the blend system are simplicity of preparation and ease of control of physical properties by compositional change [6]. However, the film properties depend upon the miscibility of the blend [7].

Among the polymer electrolytes, those based on polyvinyl alcohol (PVA) have attracted many researchers due to their good electrical and mechanical properties. Most of the commercial PVA samples have been prepared by hydrolyzing the poly(vinyl acetate). Due to the

presence of hydroxyl groups, the interchain hydrogen bond of PVA has been developed. This causes the high melting point and good mechanical stability of PVA. Yang and Pavani reported the PVA-based polymer electrolytes for electrochemical cell applications [8, 9].

Polyvinyl pyrrolidone (PVP) was selected as the second polymer for preparing polymer blend with PVA, because of its unique properties. First, PVP is an amorphous polymer that possesses high glass transition temperature (T_g) because of the presence of the rigid pyrrolidone group, which can permit faster ionic mobility compared with other semi-crystalline polymers. Second, it forms a variety of complexes with various inorganic salts due to the presence of carbonyl group (C=O) in the side chains of PVP [10, 11]. Another advantage of using PVP is that it can be thermally cross linked [12], resulting in outstanding thermal stability and mechanical strength of the blend material.

The presence of hydroxyl and carbonyl groups in the structure of PVA and PVP acts as the electron pair donors that enable complexation with metal ions. Moreover PVA and PVP have good film forming properties, and are cheap, non-toxic, and bio-degradable. The polyblend (PVA–PVP) is a potential material having a very high dielectric strength, good charge storage capacity, and dopant-dependent electrical and optical properties. A literature survey reveals that some work has been reported on conductivity studies of (PVA–PVP) polymer blend [13–15].

A lot of exploratory research has been made on monovalent salt systems like Li salts [16–18]; very little attention has been given to the polymer electrolytes based on PVA–PVP blend in which multivalent cations are the mobile species. Magnesium metal possesses a number of characteristics that make it attractive as a negative electrode material for rechargeable batteries, including its low cost, relative abundance, high safety, ease of handling, and low toxicity which allows for urban waste disposal [19]. In view of negligible hazards and enhanced safety, studies of rechargeable magnesium batteries are expected to have a wide scope in the future [20, 21]. There have been some studies on the solid polymer electrolytes based on magnesium salts [22–25]. The conductivity obtained for magnesium salt systems is comparable with the lithium salt systems [26].

In the present work, the Mg^{2+} ion conducting polymer blend electrolytes based on PVA and PVP complexed with $Mg(NO_3)_2$ have been prepared by solution cast technique. The polymer blend electrolytes have been characterized by X-ray diffraction (XRD), Fourier transform infrared (FTIR), differential calorimetry scanning (DSC), alternating current (AC) impedance spectroscopic analysis, and battery discharge studies.

Experimental

Polymer electrolyte preparation

PVA from CDH, India, which has molecular weight of 1,25,000, and PVP from CDH, India, with molecular weight of 40,000, were used as received. Equal quantity of PVA and PVP (50/50) by weight was added to doubly distilled water with stirring the solution at room temperature (303 K) to complete dissolution. Required quantity (0, 10, 20, 30, and 40 wt.%) of $Mg(NO_3)_2$ was also dissolved in doubly distilled water and added to the polymeric solution with continuous stirring. The solution was poured onto cleaned Petri dishes and dried in oven at 40 °C for 5 days to ensure removal of the solvent traces. After drying, the films were peeled from Petri dishes and kept in vacuum desiccators until use. The interactions between the polymers and salt have been shown in Scheme 1.

Characterization

In order to investigate the nature of these polymer electrolyte films, WAXD patterns were recorded in the diffraction angular range 10–60° 2θ by a Philips X'Pert PRO (Almelo, The Netherlands) diffractometer, working in the reflection geometry and equipped with a graphite monochromator on the diffracted beam (CuKα radiation). Infrared spectra profiles were obtained using a SHIMADZU-8000 FTIR spectrophotometer in the range 400–4,000 cm^{-1} in the transmittance mode at room temperature. The thermal response was studied by differential scanning calorimetry (TA Instruments mod. 2920 calorimeter) in the static nitrogen atmosphere at a heating rate of 5 °C/min in the temperature range 5 to 120 °C. Impedance measurements were carried out using HIOKI 3532-50 LCR Hitester over a frequency range 100 Hz to 1 MHz.

The transference number measurements were made using Wagner's DC polarization technique. Using the polymer electrolyte films, solid-state electrochemical cells have been fabricated with the configuration Mg/(PVA–PVP–$Mg(NO_3)_2$)/(I_2+C+electrolyte) under a constant load of 100 kΩ.

Results and discussion

XRD studies

In order to investigate the influence of the concentration of $Mg(NO_3)_2$ salt on crystallinity of polymer blend electrolytes, XRD studies were performed for pure PVA, 50PVA–50PVP, and 50PVA–50PVP–$x$wt.% of $Mg(NO_3)_2$ (x=0, 10, 20, 30, and 40) complexes which is shown in Fig. 1. A comparison of

Scheme 1 Possible interaction between polymers and salt

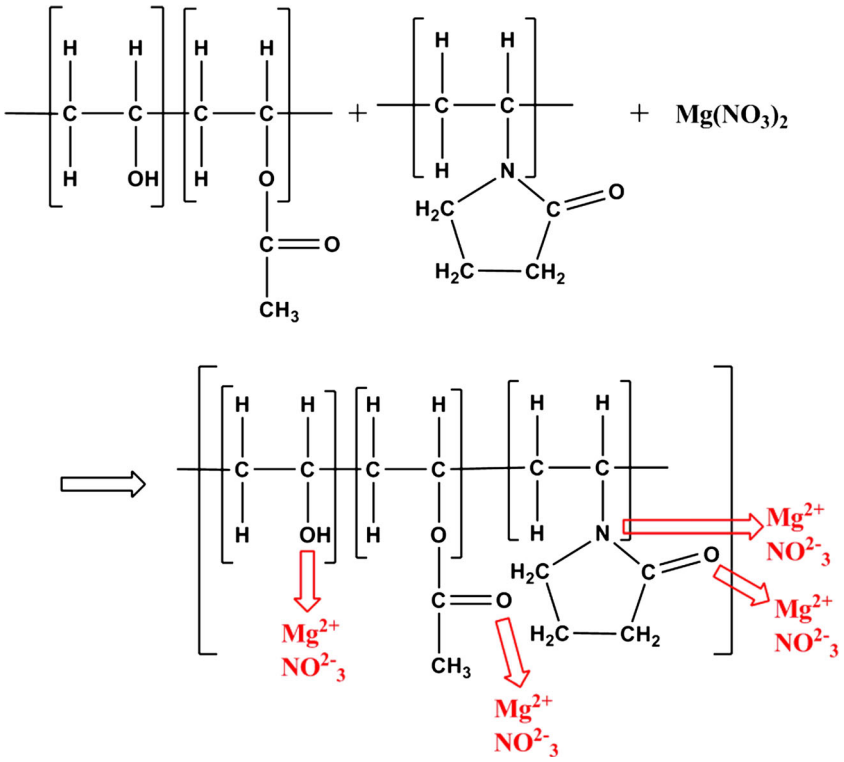

the spectra of PVA–PVP–$Mg(NO_3)_2$ films with those of pure PVA, PVA-PVP, and $Mg(NO_3)_2$ salts reveals the following:

The XRD pattern of pure PVA polymer film shows a broad peak around 19.7°. The PVA peak decreased in intensity with the addition of PVP. There is a decrease in the relative intensity of the apparent peaks with increasing magnesium salt concentration. These results can be interpreted in terms of the Hodge et al. criterion which has established a correlation between the height of the peak and the degree of crystallinity [27]. They reported that the intensity of XRD pattern decreases as the amorphous nature increases with the addition of dopant. For the filled samples, it is clearly observed that the incorporation of $Mg(NO_3)_2$ into the polymeric matrix for the polymer blend causes increase in the amorphous region of the samples, which is responsible for greater ionic diffusivity resulting in high ionic conductivity. This behavior demonstrates that complexation between the filler and the polymers which takes place in the amorphous region. All the diffraction peaks for $Mg(NO_3)_2$ are absent in the complexes. This indicates complete dissolution of the salt in the polymer matrix and hence complexation.

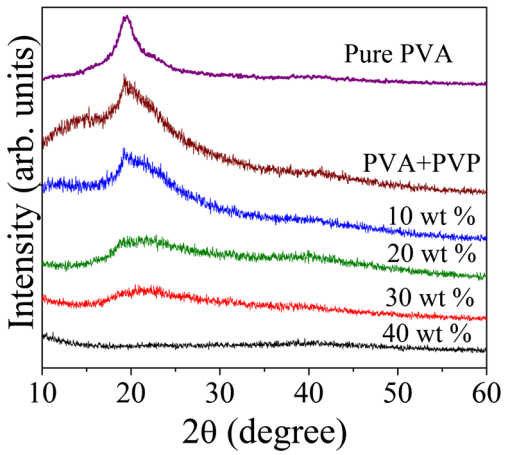

Fig. 1 X-ray diffraction patters of pure PVA, 50PVA–50PVP and 50PVA–50PVP–*x*wt.% of $Mg(NO_3)_2$ (*x*=10, 20, 30, and 40)

FTIR analysis

Infrared spectroscopy has been used to identify interactions between polymer blend and magnesium salt. FTIR spectroscopy is very sensitive to the formation of hydrogen bonds [28]. Figure 2a–e shows FTIR transmission spectra of pure PVA, pure PVP, pure $Mg(NO_3)_2$, PVA-PVP (50–50) blend, and 30 wt.% of $Mg(NO_3)_2$ doped 50PVA–50PVP blend recorded at room temperature in the region 400–4,000 cm^{-1}. FTIR absorption band positions and the assignments of all prepared samples are listed in Table 1.

The characteristic predominant O–H stretching vibration band of pure PVA at 3,436 cm^{-1} has been displaced towards lower wave number in the blend polymer electrolyte system. The peaks at 2,925 and 853 cm^{-1} assigned to C–H asymmetric stretching and C–H rocking of pure PVA, respectively, is shifted in the blend polymer complex system. The band at about 1,098 cm^{-1} corresponds to C–O stretching of acetyl

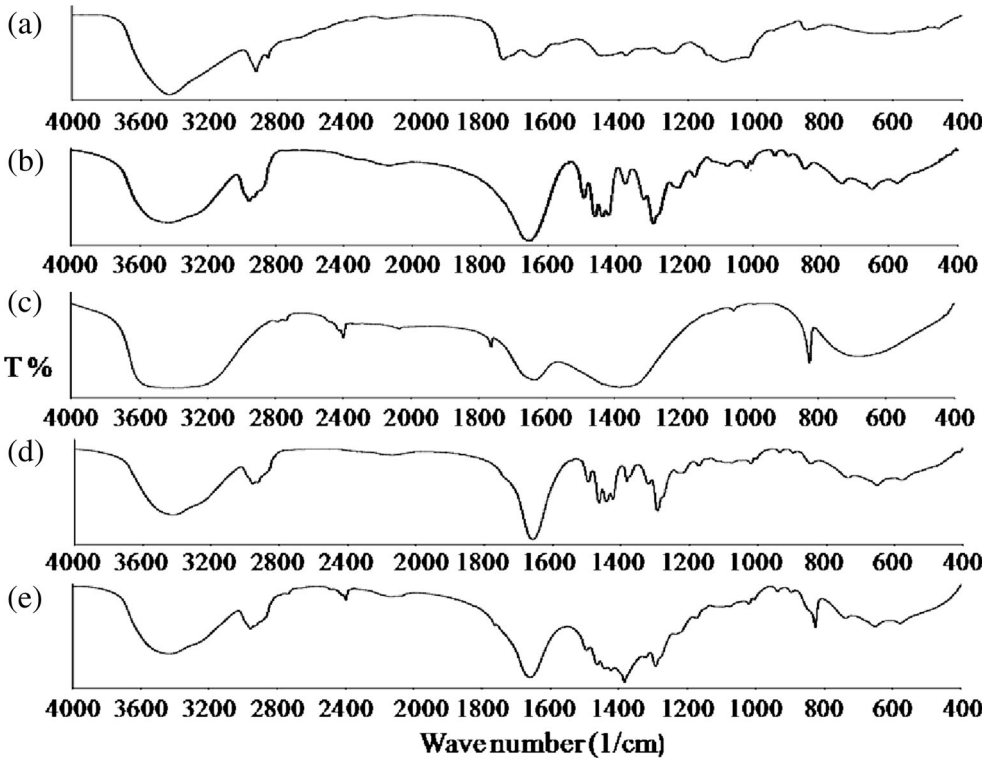

Fig. 2 FTIR spectra of **a** pure PVA, **b** pure PVP, **c** pure $Mg(NO_3)_2$, **d** PVA-PVP (50–50), **e** PVA–PVP–$Mg(NO_3)_2$ (50–50–30)

groups present on the PVA backbone. This peak is shifted in the blend polymer complex system.

Figure 2b for pure PVP shows a small absorption band at about 1,496 cm^{-1} that is assigned to the characteristic vibration of C=N (pyridine ring) [29]. The absorption band at about 935 cm^{-1} due to the out-of-plane rings C–H bending [30]. These peaks shifted to lower wave numbers in polymer blend systems. The vibrational band at about 1,655 cm^{-1} corresponds to C=C stretching of PVP [29]. This peak shifted to higher wave number in the polymer blend systems. The peak around 2,397 cm^{-1} of $Mg(NO_3)_2$ is present in the 30 wt.% of $Mg(NO_3)_2$ doped polymer blend system. The above changes in the characteristic vibrational frequencies of pure PVA, pure PVP, and $Mg(NO_3)_2$ in the blended polymer electrolyte system reveal the interaction between the polymers and magnesium ions.

Table 1 FT-IR absorption bands positions and their assignments

Vibrational frequency (cm^{-1})	Band assignment
3,436	O–H stretching
2,925	C–H asymmetric stretching
1,655	C=C stretching
1,496	C=N (pyridine ring)
1,098	C–O stretching
935	Out of plane ring C–H bending
853	C–H rocking

DSC analysis

Thermal techniques are the convenient tool to determine the physical and chemical changes such as phase transitions, glass transition temperatures (T_g), and melting parameters (melting point T_m, thermal decomposition temperature T_d, enthalpy of fusion H_f). A temperature range of 5–120 °C at a heating rate of 5 °C/min was utilized under nitrogen atmosphere. The thermal properties of pure PVA–PVP blend and their complexes were examined by DSC to estimate how the glass transition temperature of the prepared films were affected by the different concentrations of $Mg(NO_3)_2$ as shown in Fig. 3.

The values of glass transition temperature are mentioned in Table 2.The value of T_g observed for pure PVA is 85 °C [23]. After blending of PVA with PVP, the value of T_g decreases. Pure PVA–PVP curve shows a broad endothermic transition (at about 72.25 °C) attributed to T_g relaxation process resulting from micro-Brownian motion of the main chain backbone. The presence of a single glass transition indicates miscibility in the system [31]. The broad transition may be assigned to the α-relaxation associated with the crystalline regions. The position of T_g for PVA–PVP blends filled with different filling levels of $Mg(NO_3)_2$ was slightly shifted toward temperatures lower than this of the pure PVA–PVP blend. The significant T_g decreases with increasing dopant concentration may be the reduced dipole interactions in its homo polymers. The peak around 82° at high salt concentration (40 wt.% of $Mg(NO_3)_2$) represents the melting point of

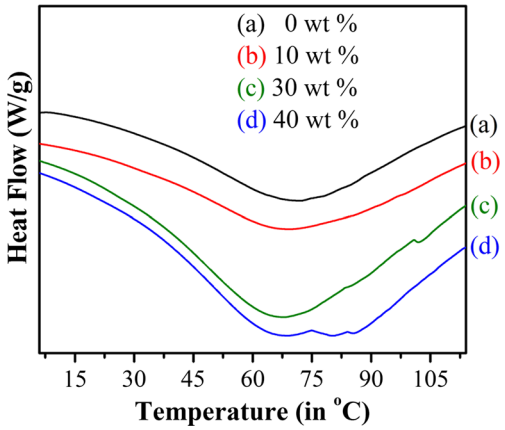

Fig. 3 DSC curves of 50PVA–50PVP–*x*wt.% of $Mg(NO_3)_2$ **a** 0 wt.%, **b** 10 wt.%, **c** 30 wt.% and **d** 40 wt.%

the $Mg(NO_3)_2$ salt. By analyzing the thermograms, it is observed that there is decrease in glass transition temperature with increase in Mg salt concentration, which means increase the amorphous nature and conductivity value with increasing Mg salt, which was confirmed by XRD and conductivity studies.

Impedance analysis

Impedance spectroscopy is employed to establish the conduction mechanism, observing the participation of the polymeric chain, mobility, and carrier generation processes. The conductivities of the polymer complexes were calculated from the bulk resistance obtained by the intercepts of the typical impedance curves for various temperatures. The impedance curves of (PVA–PVP–$Mg(NO_3)_2$) (50–50–30) system at different temperatures are shown in Fig. 4.

The complex impedance plots show two well-defined regions: the semicircle observed in the high frequency region, which is due to the bulk effect of the electrolytes, and the linear region, which, in the low frequency range, is attributed to the effect of the blocking electrodes. The disappearance of the semicircular portion in the impedance curve at high frequencies leads to a conclusion that the current carriers are ions, and this leads one to further conclude that the total conductivity is mainly the result of ionic conduction [32]. The ionic conductivities were calculated using the relation $\sigma = L/R_b A$, where L is the thickness, R_b is bulk resistance, and A is the known area of the electrolyte film.

Table 2 T_g values of PVA–PVP–$Mg(NO_3)_2$ polymer electrolyte films

S. no.	Sample	T_g in (°C)
1	Pure PVA-PVP	72.25
2	50–50–10 wt%	69.51
3	50–50–30 wt%	66.79
4	50–50–40 wt%	69.12

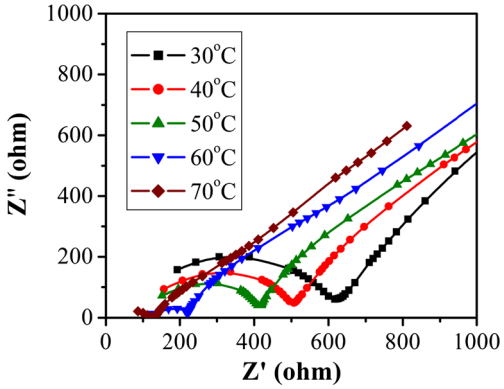

Fig. 4 Complex impedance plots for the (PVA–PVP–$Mg(NO_3)_2$) (50–50–30) polymer blend electrolyte at different temperatures

Conductivity analysis

The value of ionic conductivity for pure PVA is 5.9×10^{-9} S/cm. After blending of PVA with PVP, this value of ionic conductivity increases to 2.96×10^{-8} S/cm. The effect of magnesium salt concentrations in the polymer blend matrix on the logarithmic scale conductivity is shown in Fig. 5. It can be seen from the figure that the ionic conductivity increases with the increase in magnesium salt concentration up to 30 wt.% of $Mg(NO_3)_2$. The polymer electrolyte obtained from 30 wt.% of $Mg(NO_3)_2$ with PVA–PVP polymer blend has high ionic conductivity of 3.44×10^{-5} S/cm. This value is higher than the PVA blend with PVP and optimum conductivity of PVA–$Mg(NO_3)_2$ ($\sigma=7.36\times10^{-7}$ S/cm) [23]. The conductivity increases initially with increasing salt concentration as the number of charge carriers increases. Beyond this concentration, the ionic conductivity decreases. This is due to the formation of ion pairs and ion triplet, which causes constraint in the polymer segmental motion and also retards the ionic mobility due to the increase in crystallinity nature of polymer electrolyte [33].

Figure 6 shows the variation of conductivity as a function of temperature for pure (PVA–PVP) and for different

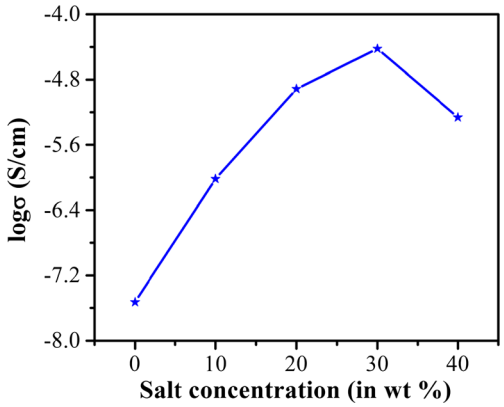

Fig. 5 Effect of the concentration of magnesium nitrate on the conductivity of 50PVA–50PVP blend at room temperature (303 K)

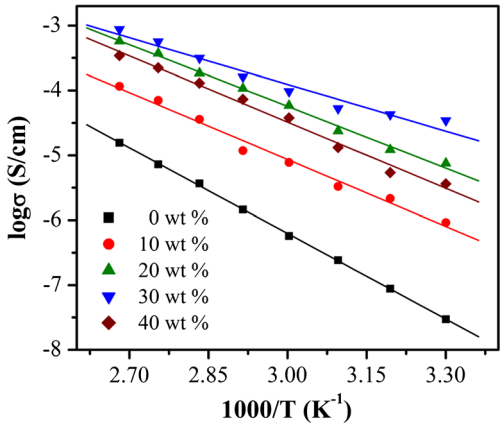

Fig. 6 Temperature-dependent conductivity of 50PVA–50PVP–*x*wt.% of $Mg(NO_3)_2$ (*x*=0, 10, 20, 30, and 40) polymer blend electrolytes

compositions of (PVA–PVP–$Mg(NO_3)_2$) polyblend in the temperature range 303–373 K. The conductivity was found to increase with increasing temperature in both pure and $Mg(NO_3)_2$ complexed polyblend electrolyte system. The conductivity–temperature plots followed an Arrhenius behavior throughout the temperature range. The variation of conductivity (σ) with temperature (T) can be fitted to the relation (Eq. 1) [34].

$$\sigma = \sigma_0 \exp\left(-E_a \Big/ kT\right) \tag{1}$$

where σ_0 is a constant, k, the Boltzmann constant, and E_a, the activation energy. The activation energy values were 0.87, 0.68, 0.63, 0.475, and 0.567 eV for pure and 10 %, 20 %, 30 %, and 40 % $Mg(NO_3)_2$ complexed PVA–PVP films, respectively. The activation energy value of $Mg(NO_3)_2$ complexed films decreases compared with pure PVA–PVP. The low activation energy value is obtained for PVA–PVP–30 wt.% of $Mg(NO_3)_2$ composition. As increase in temperature leads to an increase in conductivity, this is only expected because, as the temperature increases, the polymer expands to produce free volume, which leads to enhanced ionic mobility and polymer segmental mobility. The conductivity variation of polymer electrolytes obeys the Arrhenius behavior which describes the transport properties in a viscous polymer matrix [35].

The variation of the ac conductivity with frequency for different $Mg(NO_3)_2$ concentrations with PVA–PVP blend at 303 K and for (PVA–PVP–$Mg(NO_3)_2$) (50–50–30) system at different temperatures are shown in Fig 7a and b, respectively. From the plot in Fig. 7a, it is observed that the conductivity increases from 2.94×10^{-8} to 3.41×10^{-5} S/cm with increase of $Mg(NO_3)_2$ concentration up to 30 wt.% and after which the conductivity decreases. The frequency-dependent AC conductivity of the polymer electrolyte is described by

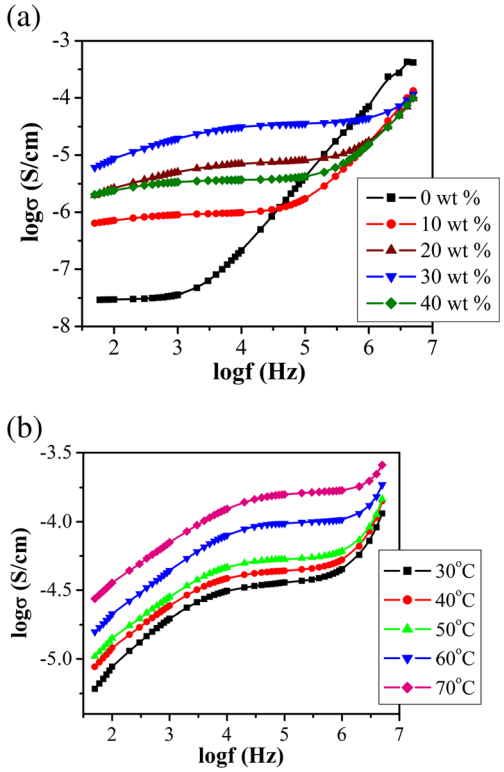

Fig. 7 **a** Conductance spectra of 50PVA–50PVP–*x*wt.% of $Mg(NO_3)_2$ (*x*=0, 10, 20, 30, and 40) polymer blend electrolytes with different salt concentrations at 303 K. **b** Conductance spectra of 50PVA–50PVP–30 wt.% of $Mg(NO_3)_2$ polymer blend electrolyte at different temperatures

Almond and West formalism [36],

$$\sigma(\omega) = \sigma_{dc} + A\omega^n \tag{2}$$

where A and n are material parameters, $0<n<1$, σ_{dc} is dc ionic conductivity, and ω is the angular frequency. The plots shows three regions: The first one is the low frequency dispersion region observed which can be ascribed to the space charge polarization at the blocking electrodes. The second region corresponds to the frequency-independent plateau region. The conductivity is found almost frequency-independent in this region, and the extrapolation of the plot to zero frequency gives the value of DC conductivity at all temperatures. From Fig. 7b, as temperature increases, the frequency-independent conductivity region decreases, and thus, the polarization effect becomes prominent. The high frequency conductivity dispersion is prominent at lower temperatures.

Transference number studies

The transference numbers corresponding to ionic (t_{ion}) and electronic (t_{ele}) transport have been calculated for (PVA–PVP–$Mg(NO_3)_2$) (50–50–30) polymer blend electrolyte film using Wagner's DC polarization technique

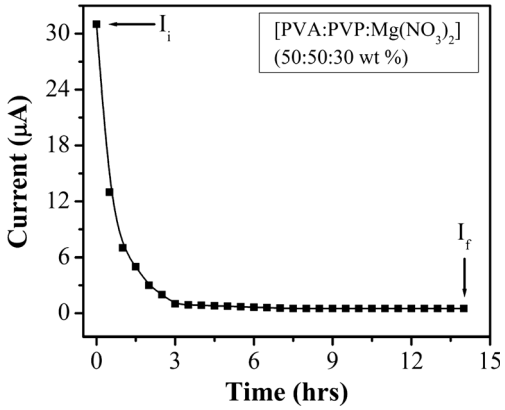

Fig. 8 Polarization current versus time plot of 50PVA–50PVP–30 wt.% of $Mg(NO_3)_2$ polymer blend electrolyte film

[37]. In this method, the DC current is monitored as a function of time on the application of fixed DC voltage across the Mg/(PVA–PVP–$Mg(NO_3)_2$) (50–50–30)/C cell. After applying 1.5 V, the current versus time plot was obtained, which is shown in Fig. 8 for a (PVA–PVP–$Mg(NO_3)_2$) (50–50–30) electrolyte. The transference number has been calculated from the polarization current versus time plot using Eq. 3

$$t_{\text{ion}} = (\mathrm{I_i} - I_{\mathrm{f}}) \Big/ I_{\mathrm{i}} \tag{3}$$

where I_i is the initial current and I_f is the final residual current. The ionic transference number (t_{ion}) for (PVA–PVP–$Mg(NO_3)_2$) (50–50–30) polymer blend electrolyte system is found to be ~0.98. This suggests that the charge transport in this electrolyte film is predominantly due to ions.

Discharge studies

Using (PVA–PVP–$Mg(NO_3)_2$) (50–50–30) blend polymer electrolyte film, solid-state electrochemical cell

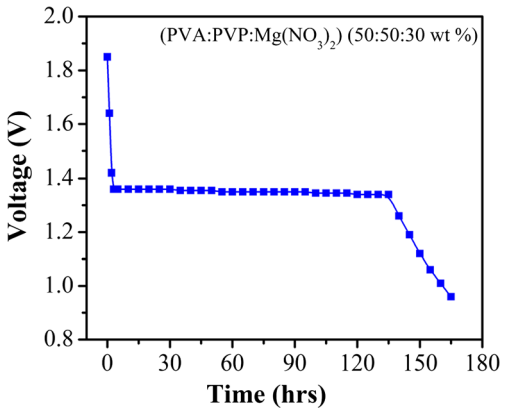

Fig. 9 Discharge characteristic plot of 50PVA–50PVP–30 wt.% of $Mg(NO_3)_2$ electrochemical cell for a constant load of 100 kΩ

Table 3 Cell parameters of (PVA–PVP–$Mg(NO_3)_2$) electrolyte cell for a constant load of 100 kΩ

Cell parameters	Mg/[PVA–PVP–$Mg(NO_3)_2$]/(I_2+C+electrolyte)
Cell weight	1.47 g
Area of the cell	1.33 cm^2
Open circuit voltage (OCV)	1.85 V
Discharge time for plateau region	136 h
Current density	13.91 μA/cm^2
Discharge capacity	2.442 mAh
Power density	17.12 mW/kg
Energy density	2825 mW h/kg

was fabricated in the configuration: Mg (anode)/(PVA–PVP–$Mg(NO_3)_2$) (50–50–30)/(I_2+C+electrolyte) (cathode). Magnesium metal was used as the negative electrode, and a mix of iodine (I_2), graphite (C), and electrolyte in the ratio 5:5:1 as the positive electrode. The discharge characteristics of the cell Mg/(PVA–PVP–$Mg(NO_3)_2$) (50–50–30)/(I_2+C+electrolyte) at ambient temperature for a constant load of 100 KΩ is shown in Fig. 9. The initial sharp decrease in voltage of this cell may be due to polarization and/or formation of a thin layer of magnesium salt at the electrode/electrolyte interface. The open-circuit voltage (OCV) and other cell parameters for this cell are given in Table 3. The cell parameters of the present polymer electrolyte system is comparable with the cell parameters reported for other cells, thus offering an interesting option of application of these electrolytes for solid state batteries.

Conclusion

Solid polymer blend electrolytes based on polyvinyl alcohol and polyvinyl pyrrolidone complexed with $Mg(NO_3)_2$ have been prepared by solution cast method. Their complexation has been characterized by XRD and FTIR techniques. The XRD study reveals the amorphous nature of the polymer blend electrolytes. FTIR studies showed that co-existence of vibrational bands correspond to PVA and PVP and confirm the miscibility of the blend. DSC thermograms show the decrease of T_g with the increase of $Mg(NO_3)_2$ content. The maximum value of ionic conductivity for the PVA–PVA–$Mg(NO_3)_2$ (50–50–30) system is 3.44×10^{-5} S/cm at 30 °C. The temperature-dependent conductivity of polymer electrolytes obeys the Arrhenius behavior. The conducting species in the polymer electrolyte system was found to be predominantly

ions. From electrochemical analysis, it could be seen that the solid polymer electrolyte system using PVA–PVP is an effective tool for improving the properties of magnesium polymer secondary batteries.

References

1. Scrosati B (1993) Application of electroactive polymers. Chapman and Hall, London
2. Polu AR, Kumar R, Joshi GM (2014) Ionics 20:675–679
3. Serhat V, Metin AK, Cihangir T, Idris MA, Levent T (2006) Solid State Sci 8:1477–1483
4. Ratner MA, Shriver DF (1988) Chem Rev 88:109–124
5. Cherng JY, Munshi MZA, Owens BB, Smyrl WH (1988) Solid State Ionics 28:857–861
6. Rocco AM, Pereira RP, Felisberti MI (2001) Polymer 42:5199–5205
7. Abdelrazek EM, Elashmawi IS, El-Khodary A, Yassin A (2010) Curr Appl Phys 10:607–613
8. Yang CC, Lin SJ, Wu GM (2005) Mater Chem Phys 92:251–255
9. Pavani Y, Ravi M, Bhavani S, Sharma AK, Rao VVRN (2012) Polym Eng Sci 52:1685–1692
10. Feng H, Feng Z, Shen L (1993) Polymer 34:2516–2519
11. Zhang X, Takegoshi K, Hikichi K (1992) Polymer 33:712–717
12. Zieba JJ, Zhang Y, Prasad PN (1992) Sol–Gel Opt II 1758:287
13. Subba Reddy CV, Sharma AK, Rao VVRN (2006) Polymer 47: 1318–1323
14. Rajeswari N, Pandian SS, Karthikeyan S, Sanjeeviraja C, Iwai Y, Kawamura J (2013) Ionics 19:1105–1113
15. Hatta FF, Yahya MZA, Ali AMM, Subban RHY, Harun MK, Mahamad AA (2005) Ionics 11:418–422
16. Chithra MM, Kesavan K, Rajedran S (2014) Ionics 20:439–443
17. Aravindan V, Vickraman P (2009) Polym Eng Sci 49:2109–2115
18. Li Y, Xiao W, Li X, Miao C, Guo H, Wang Z (2014) Ionics. doi:10.1007/s11581-014-1081-8
19. Gregory TD, Hoffman RJ, Winterton RC (1990) J Electrochem Soc 137:775–780
20. Novak P, Imhof R, Haas O (1999) Electrochim Acta 45:351–367
21. Aurbach D, Lu Z, Schechter A, Gofer Y, Gizbar H, Turgeman R, Cohen Y, Moshkovich M, Levi E (2000) Nature 407:724–727
22. Polu AR, Kumar R (2013) Int J Polym Mater 62:76–80
23. Polu AR, Kumar R (2013) Chin J Polym Sci 31:641–648
24. Polu AR, Kumar R (2013) Adv Mat Lett 4:543–547
25. Polu AR, Kumar R (2011) Bull Mater Sci 34:1063–1067
26. Matsumoto M, Uno T, Kubo M, Itoh T (2013) Ionics 19:615–622
27. Hodge RM, Edward GH, Simon GP (1996) Polymer 37:1371–1376
28. Rajendran S, Sivakumar M, Subadevi R (2004) Mater Lett 58: 641–649
29. Abdelrazek EM, Elashmawi IS, Ragab HM (2008) Physica B 403: 3097–3104
30. Wu KH, Wang YR, Hwu WH (2003) Polym Degrad Stab 79:195–200
31. Walsh DJ (1989) 'Polymer Blends', in comprehensive polymer science, vol. 2, Booth C (eds), Price C, Pergamon Press, Oxford, UK, pp 135–154
32. Jacob MME, Prabaharan SRS, Radhakrishna S (1997) Solid State Ionics 104:267–276
33. Subramania A, Kalyana Sundaram NT, Sukumar N (2005) J Power Sources 141:188–192
34. Maissel LI, Glang R (1970) Handbook of thin film technology. McGraw-Hill, New York
35. Aravindan V, Vickraman P (2007) Solid State Sci 9:1069–1073
36. Almond DP, West AR (1987) Solid State Ionics 23:27–35
37. Wagner JB, Wagner C (1957) Chem Phys 26:1597–1601